Control Volume Finite Difference On Adaptive Meshes

S. K. Khattri, G. E. Fladmark and H. K. Dahle

Department of Mathematics, University Bergen, Norway.
`sanjay@mi.uib.no`

Summary. In this work we present a finite volume discretization of an elliptic boundary value problem on adaptively refined meshes. This problem is important in many practical applications, e.g. porous media flow. We propose an error indicator functional which is used to select elements that should be refined. Two numerical examples are provided to demonstrate the potential of the proposed refinement strategy.

1 Introduction

Finite volume [6] and finite element [2, 3, 4] are widely used methods for discretizing partial differential equations. Behaviour of finite element methods on adaptive meshes is well understood and studied, e.g., [2, 3, 4], whereas finite volume method seems to be less studied. In this paper, we will consider a cell centered finite volume method also known as control volume finite difference method (CVFD) [6, 9]. Finite volume methods are popular for example in the porous media community since they are based on conservation principles and honour the continuity of fluxes. There are different ways of expressing the fluxes through the boundaries of a cell which give rise to different formulations like the two point flux approximation methods (TPFA) and the multi point flux approximation methods (MPFA), [1, 6]. In this work, we will use a TPFA method. Consider the numerical solution of the following elliptic boundary value problem using adaptive meshes:

$$-\nabla \cdot (\boldsymbol{K} \, \nabla p) = f(x, y) \qquad \text{in} \quad \Omega, \tag{1}$$

$$p(x, y) = p^{\mathrm{D}} \qquad \text{on} \quad \partial\Omega. \tag{2}$$

Here, Ω is a polyhedral domain in $\mathrm{I\!R}^2$, the source function f is assumed to be in $L^2(\Omega)$, and $\boldsymbol{K}$ is symmetric and uniformly positive definite tensor which may depend on the spatial coordinate. In porous media flow, the unknown function $p = p(x, y)$ represents the pressure of a single fluid, and $\boldsymbol{K}$ is the

permeability of the porous medium Ω. The rest of the paper is organised as follows: In Section 2, a simple criterion for adaptive refinement is proposed, and an algorithm for an adaptive meshing strategy is given. In Section 3, we give two numerical examples. In the first example, the permeability $\boldsymbol{K}$ is constant while the source exhibits a huge variability. In the second example, the medium properties represented by the permeability $\boldsymbol{K}$ are discontinuous. In both cases an analytic solution is known and the error for the discrete solutions on adaptively and uniformly refined meshes can be computed. These errors are then compared for meshes that possess the same degree of freedom (DOF). Finally in Section 4, we provide some concluding remarks.

2 Adaptive Criteria and Adaptive Algorithm

Adaptive refinement are feed-back based discretizations (**Solve → Estimate → Refine/Coarse**). Thus we need criterion for selecting finite volumes/cells in the mesh for further refinement. Ultimately these methods construct a sequence of meshes that may converge to an optimal mesh (the most accurate solution at a fixed cost or lowest computational effort for a given accuracy). Generally most of the error occurs in areas where the solution exhibits large gradients, varying curvature or high source variability [2, 3, 4]. Based on these heuristics we propose the following error indicator for a cell i in the mesh:

$$\eta_i = \alpha \, \|p_h\|_{L_2(\Omega_i)} + \alpha_G \, \eta_G + \alpha_F \, \eta_F + \alpha_S \, \eta_S. \tag{3}$$

Here, α, α_G, α_F and α_S are weights belonging to the interval $[0, 1]$, and η_G, η_F and η_S are given as follows:

$$\eta_G := \|\nabla p_h\|_{L_2(\Omega_i)}, \tag{4}$$

$$\eta_F := \|(\boldsymbol{K} \, \nabla p_h) \cdot \hat{\mathbf{n}}\|_{L_2(\partial \Omega_i)}, \tag{5}$$

$$\eta_S := \|f\|_{L_2(\Omega_i)}. \tag{6}$$

In these formulas, we will use least square fitting to approximate the gradient, ∇p_h, of the discrete pressure p_h. An error error indicator need not to represent the error very accurately [3], they just need to select the elements for further refinement. An element i in the mesh will be refined if $\frac{\eta_i}{\max_j \eta_j} \geq \delta$ $(0 \leq \delta \leq 1)$. Thus, $\delta = 0$ means a uniform refinement and $\delta = 1$ means that the algorithm will refine a single element per iteration. None of these end point values may be optimal. A trade off between uniform refinement and refining a single element at a time is obtained by choosing $\delta = 0.5$. This value has also been suggested in the literature, e.g., [4]. In general the choice of an optimal set of parameters δ, α, α_G, α_F and α_S is a difficult task. In this work, we have chosen these parameters based on experience with the specific problems. Optimal choice of these numbers will be investigated in future research. It should be noted that if α_S and α_F are equal to zero then the indicator (3) is similar to the indicator

proposed in [4] for an Adaptive Discontinuous Galerikin Method, whereas if α and α_G is equal to zero then the indicator is similar to the one given in [2, 3] for an adaptive finite element method. The overall algorithm we are using is presented in Algorithm 1. This adaptive algorithm works on the principle of equally distributing the adaptivity index over all cells in the mesh. For a cell centered finite volume method the degrees of freedom (DOF) are equal to the number of cells in the mesh. In Algorithm 1, the refinement is stopped at a fixed maximum DOFs. In general an a posteriori error estimator should be added as a stopping criterion, (cf. [4, 7, 10]).

Algorithm 1: Adaptive Algorithm.

Mesh the domain;
while $DOF < DOF_{\max}$ **do**
    Discretize the PDE over the mesh by the CVFD;
    Solve the discrete system;
    forall *elements j in the mesh* **do**
        if $\eta_j / \max_i \eta_i \geq \delta$ **then**
            Refine the element j in the mesh;
        end
    end
    Form a new mesh;
end

---

3 Numerical Examples

Let p^k denotes the exact solution for the pressure at the center of cell k, and p_h^k denotes the discrete pressure obtained by the finite volume approximation for the same location. Then the discrete error e in the L_2 norm for a mesh can be expressed as:

$$\|e\|_{L_2} := \left(\sum_{\text{cells}} \left[p^k(x) - p_h^k(x) \right]^2 \, \Omega_k \right)^{1/2}. \tag{7}$$

Here, the summation is to be taken over all the cells/finite volumes in the mesh. The CVFD approximation of the equation (1) subject to the boundary condition (2) using a two point flux approximation (TPFA) leads to symmetric positive definite linear systems. To solve these systems, we are using the ILU preconditioned conjugate gradient (CG) solver with a tolerance of 1×10^{-10}.

3.1 Example 1

Let the domain be $\Omega = (0,1) \times (0,1)$, and the permeability be the identity tensor $\boldsymbol{K} = \boldsymbol{I}$. We enforce the source term $f = f(x,y)$ such that the analytical

solution to Equation (1) is given by

$$u(x, y) = 0.0005 \left[x \ (x - 1) \ y \ (y - 1) \right]^2 e^{10 \, (x^2 + y^2)}. \tag{8}$$

Note that this solution is consistent with the zero Dirichlet boundary condition (2). Furtheremore, taking the Laplacian of (8) shows that the source term exhibits a huge variability inside the domain and even within the cells. For this problem we found that $\delta = 0.5$, $\alpha = 0.0$, $\alpha_G = 0.10$, $\alpha_F = 0.90$ and $\alpha_S = 1.0$ was a good choice of parameters for the indicator functional (3). However, other choices may work even better. Figures 3 reports the outcome of a numerical experiment comparing the discrete solutions on an adaptively refined mesh and a uniform mesh. The degrees of freedom (DOF) associated with the meshes depicted in these figures are approximately the same. However, the L_2 errors in the solutions on adaptive and uniform meshes are 8.91×10^{-4} and 3.7×10^{-3}, respectively. Thus, the error of the solution on the adaptively refined mesh is much smaller compared to the solution on the uniform grid. In Figure 3.1, we have plotted the error versus DOF for solutions on adaptively refined meshes and for uniform meshes. From this plot we get that $\|e\| \sim \mathrm{DOF}^{-p/2}$ with $p \approx 2$ on the adaptive meshes, which is quasi optimal in the sense of [7, 10]. Since the solution is smooth, we expect the advantage of adaptive refinement to be largest for coarser grids, while this advantage should be reduced compared to a uniform refinement for finer grids. This is indeed what can be observed in Figure 3.1.
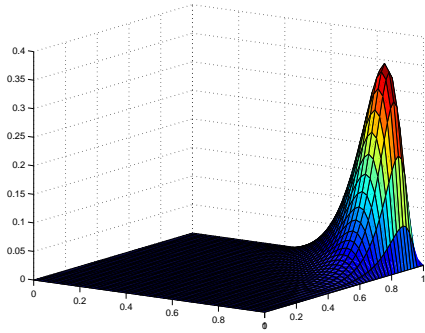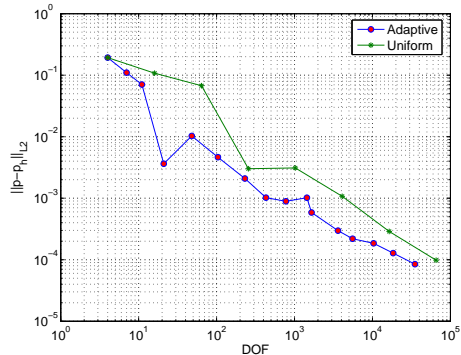

Fig. 1. (Example 3.1) Exact solution.

Fig. 2. (Example 3.1) L_2 error vs degrees of freedom for adaptively generated meshes and uniform meshes.
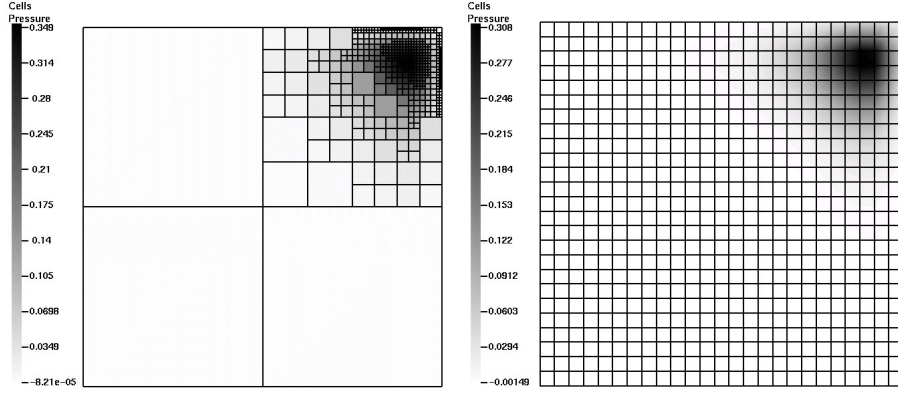
Fig. 3. (Example 3.1) Discrete solution on adaptive and uniform meshes. DOF for the adaptive mesh is 601, and DOF for uniform refinement is 625. L_2 error on adaptive mesh is 8.91×10^{-4} while on uniform mesh it is 3.7×10^{-3}.

3.2 Example 2

In porous media flow, material properties as given by the permeability is often piecewise constant. The numerical challenges introduced by the discontinuities in the permeability are difficult to handle by standard formulations, see [4, 5, 1, 6, 9]. In this example, we will investigate the behaviour of our refinement strategy for a problem with discontinuous permeability. Let $\Omega = (-1, 1) \times (-1, 1)$. We subdivided Ω into four non overlapping subregions Ω_i $i = 1 \ldots, 4$ such that $\Omega = \cup_i \Omega_i$ as shown in Figure 4. For each subregion Ω_i we associate a constant permeability $\boldsymbol{K}$, and will assume that

$$\boldsymbol{K_2} = \boldsymbol{K_4} = \boldsymbol{I} \qquad \text{and} \qquad \boldsymbol{K_1} = \boldsymbol{K_3} = R\,\boldsymbol{I}, \tag{9}$$

where R is a parameter to be determined. An analytic solution can be constructed using the polar representation

$$p(r, \theta) = r^\gamma \eta(\theta), \tag{10}$$

see [7, 10]. Let $\eta(\theta)$ be given by

$$\eta(\theta) = \begin{cases} \cos\left[(\pi/2 - \sigma)\gamma\right] \cos\left[(\theta - \pi/2 + \rho)\gamma\right], & \theta \in [0, \dfrac{\pi}{2}], \\[2mm] \cos(\rho\gamma) \cos\left[(\theta - \pi + \sigma)\gamma\right], & \theta \in [\dfrac{\pi}{2}, \pi], \\[2mm] \cos(\sigma\gamma) \cos\left[(\theta - \pi - \rho)\gamma\right], & \theta \in [\pi, \dfrac{3\pi}{2}], \\[2mm] \cos\left[(\pi/2 - \rho)\gamma\right] \cos\left[(\theta - 3\pi/2 - \sigma)\gamma\right], & \theta \in [\dfrac{3\pi}{2}, 2\pi], \end{cases} \tag{11}$$

and let the numbers R, γ, ρ and σ satisfy the nonlinear relations:

$$
\begin{aligned}
R &= -\tan\left[(\pi - \sigma)\gamma\right]\cot(\rho\gamma), \\
1/R &= -\tan(\rho\gamma)\cot(\sigma\gamma), \\
R &= -\tan(\sigma\gamma)\cot\left[(\pi/2 - \rho)\gamma\right], \\
&0 < \gamma < 2, \\
&\max\{0, \pi\gamma - \pi\} < 2\gamma\rho < \min\{\pi\gamma, \pi\}, \\
&\max\{0, \pi - \pi\gamma\} < -2\gamma\rho < \min\{\pi, 2\pi - \pi\gamma\}.
\end{aligned}
\tag{12}
$$

Then it can be shown that (10) satisfies Equation (1) with $\boldsymbol{K}$ given by (9) and $f(x, y) = 0$. Boundary conditions need to be chosen consistently with the form (10). Furthermore, it can be shown that the solution p belongs to the fractional Sobolev space $\mathbf{H}^{1+\xi}(\Omega)$ where $\xi < \gamma$ (cf. [8]). By choosing $\gamma = 0.3$, we can solve the constrained nonlinear relations (12) using Newton's iteration to get $R = 17.3476$, $\sigma = -4.4506$ and $\rho = 0.7853$. We specify the parameters for the indicator functional to be $\delta = 0.6$, $\alpha = 0.0$, $\alpha_G = 0.0$, $\alpha_F = 1.0$, $\alpha_S = 0.0$. In Figure 5, we have plotted the error in the discrete solution against the degrees of freedom for both adaptive and uniform meshes. Again we observe that the convergence on adaptive meshes are much better than for uniform refinement. We also get that $\|e\|_{L_2} \sim \mathrm{DOF}^{-p/2}$ with $p \approx 2.0$ for the solution on adaptive meshes. Because of the regularity of the solution, this convergence is also quasi optimal in the sense of [7, 10]. Finally in Figure 6 we plot the number of CG iterations (without preconditioning) vs. the DOFs for the adaptive and uniformly refined meshes. The plot shows that the uniformly refined meshes require approximately twice as many CG iterations as the adaptive refinement. This suggests that the condition number for the matrix obtained for uniform refinement is four times the condition number for the matrix obtained for adaptive refinement.
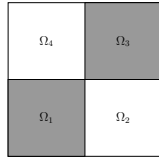

Fig. 4. (Example 3.2) Domain with discontinuous medium properties. The permeability is constant over each sub-domains i.e., $\boldsymbol{K}=\mathbf{K}_i$ in Ω_i.

4 Conclusions

In this work we have given a strategy for adaptive refinement in the setting of CVFD discretizations of boundary value problems. The mesh refinement is based on the use of an error indicator functional. We have tested the methods on two test examples. In both cases the solution has a strong local behaviour which is clearly captured by our refinement strategy. We have computed the
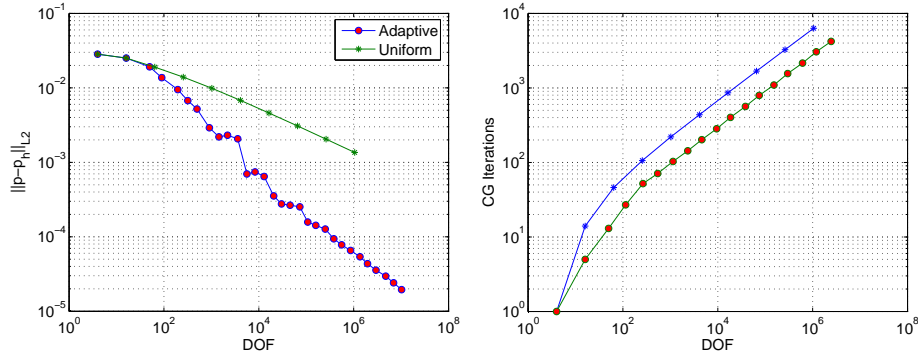
Fig. 5. (Ex. 3.2) Pressure convergence in L_2 norm for adaptive and uniform refinement.

Fig. 6. (Ex. 3.2) Number of CG Iterations (no preconditioner) vs. DOFs. Star is representing uniform refinement while circle is associated with adaptive refinement.

error in the discrete solution to obtain convergence rates. The numerical experiments suggest that convergence is quasi optimal as the mesh is adaptively refined for both the test examples. Furthermore we have compared CVFD on adaptive and uniform meshes. As expected the solutions obtained for adaptive meshes are significantly more accurate, and the system matrices are better conditioned when we employ adaptive meshes. Even though our preliminary investigations show that the proposed CVFD discretization on adaptive meshes has a great potential, many challenges remain open for further research. Most importantly we need to find better ways of selecting parameters for the indicator functional.

References

1. S.K. Khattri: Numerical tools for multi-component, multi-phase, reactive transport in porous medium. PhD Thesis, The University of Bergen, Norway (2006).
2. I. Babuska and A. Miller: A Feedback finite elment method with a posteriori error estimation: Part I. The Finite Element Method and Some Basic Properties of the a Posteriori Error Estimators. Comp. Meth. Appl. Mech. Eng., **61**, 1–40 (1987).
3. I. Babuska and W.C. Rheinboldt. Analysis of Optimal Finite Element Meshes. Math. Comp., **33**, 435–463 (1979).
4. B. Riviere: Discontinuous Galerkin Fnite Element Methods for Solving the Miscible Displacement Problem in Porous Media. PhD Thesis, The University of Texas at Austin (2000).
5. G.T. Eigestad and R.A. Klausen: On the convergence of the multi-point flux approximation O-method: Numerical experiments for discontinuous permeability. Numer. Methods Partial Differential Equations, **21**, 1079–1098 (2005).

6. I. Aavatsmark: An introduction to multipoint flux approximations for quadrilateral grids. Comput. Geosci., **6**, 405–432 (2002).
7. P. Morin, R.H. Nochetto, and K.G. Siebert: Data Oscillation and Convergence of Adaptive FEM. SIAM J. Numer. Anal., **38**, 466-488 (2000).
8. G. Strang and G. J. Fix: An Analysis of the Finite Element Method. Wiley, New York (1973).
9. M. G. Edwards and C. F. Rogers: Finite Volume Discretization with Imposed Flux Continuity for the General Tensor Pressure Equation. Comput. Geosci., **2**, 259–290 (1998).
10. Z. Chen and S. Dai: On the Efficiency of Adaptive Finite Element Methods for Elliptic Problems with Discontinuous Coefficients. SIAM J. Sci. Comput., **24**, 443–462 (2002)